

Image Cover Sheet

CLASSIFICATION

SYSTEM NUMBER

507638

UNCLASSIFIED



TITLE

MODELLING OF THE EXPLOSIVE H6

System Number:

Patron Number:

Requester:

Notes:

DSIS Use only:

Deliver to:



UNCLASSIFIED

DEFENCE RESEARCH ESTABLISHMENT
CENTRE DE RECHERCHES POUR LA DÉFENSE
VALCARTIER, QUEBEC

DREV - TM - 9802

Unlimited Distribution / Distribution illimitée

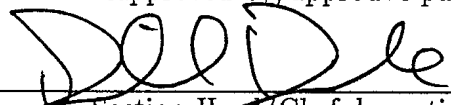
Modelling of the Explosive H6

by

G. McIntosh

March/mars 1998

Approved by/approuvé par


Section Head/Chef de section

98/01/09

Date

SANS CLASSIFICATION

UNCLASSIFIED

i

ABSTRACT

An attempt to model the shock-to-detonation behaviour of the explosive H-6 has been made. The Forest fire model of ignition was calibrated using experimental data. Simulations of polymethylmethacrylate (PMMA or plexiglas) and water gap tests were then made using DYNA2D into which the Forest fire model had been implemented. The results show that while the onset of detonation (critical gap thickness) can be predicted fairly well, the subsequent events, such as backsurface velocities of the explosive, are not accurately predicted.

RÉSUMÉ

On a effectué un essai de modélisation de la transition choc à détonation de l'explosif H-6. Le modèle d'amorçage 'Forest fire' a été étalonné à l'aide de données expérimentales. Des simulations des tests d'écart de PMMA et d'eau ont été effectuées avec le programme DYNA2D dans lequel on avait implanté le modèle 'Forest fire'. Les résultats démontrent qu'il est possible de prédire avec une précision relative le début d'une détonation (écart critique). Cependant, on ne peut pas prédire le comportement subséquent avec une grande précision.



TABLE OF CONTENTS

ABSTRACT/RÉSUMÉ	i
EXECUTIVE SUMMARY	v
LIST OF SYMBOLS	vii
1.0 INTRODUCTION	1
2.0 H6 EXPLOSIVE CHARACTERIZATION	1
3.0 MODIFIED GAP TEST SIMULATIONS	7
4.0 UNDERWATER SENSITIVITY TEST SIMULATIONS	9
5.0 COMMENTS ON THE RESULTS	13
6.0 REFERENCES	15
FIGURES 1 to 5	
TABLES I to III	



EXECUTIVE SUMMARY

Current emphasis in the detonics research is on accurate modelling of explosive behaviour. Modelling is cheaper, safer and more flexible than doing many series of experiments. However, the computational description of an explosive must be as accurate as possible before simulations of it are considered reliable. The explosive H-6 is a difficult explosive to model and, therefore, KTA 1-28 (under TTCP W-1) was set up to see how successfully various countries can deal with it. The explosive H-6 is an explosive commonly used in underwater mines and torpedo warheads.

In this work, one particular model of explosive behaviour, called the Forest fire model, was used. It was calibrated using one series of experiments and was then used to model two more sets of experiments which involved shock transfer across a gap of polymethylmethacrylate (plexiglas) or water and shock impact on a H-6 explosive sample. The behaviour of the sample was studied. In general, the onset of detonation in the sample agreed with the experiments but the subsequent effects (especially expansion velocities) were not well predicted. The discrepancy is probably due to an error in the equation of state for the explosive after ignition. A better equation of state should be used.

The results of this work will be compared with efforts from other TTCP countries and collectively, a reliable model for the modelling of H-6 may be produced. If a model becomes available, mineclearing operations in harbours by sympathetic detonation of the H6-filled mines will be easier to simulate and optimum scenarios for their destruction could be suggested.



LIST OF SYMBOLS

C	Sound speed (may be subscripted)
C_V	heat Capacity at constant Volume
P	Pressure (may be subscripted)
S	Slope in Hugoniot velocity relation (may be subscripted)
T	Temperature (may be subscripted)
V	specific Volume (may be subscripted)
α	coefficient of linear expansion
α_1, α_2	coefficients for Pop plot relation
γ_s	Grüneisen parameter for the solid explosive
κ	coefficient of isothermal compressibility
ρ	density (may be subscripted)

Subscripts

CJ	Chapman-Jouget
g	gas
H	Hugoniot
i	isentrope
o	original (ambient) conditions
p	particle
s	solid
S	Shock
VN	von Neumann

The above list is not exhaustive but does include most of the symbols used in this document.



1.0 INTRODUCTION

One of the current activities in detonics research is the modelling of explosive behaviour since it is cheaper, safer and more flexible than doing many series of experiments. However, the computational description of an explosive must be as accurate as possible before simulations of it can be considered reliable. The explosive H-6, commonly used in underwater mines and torpedo warheads, is a difficult explosive to model because of its non-ideal late time behaviour. Therefore, KTA 1-28 (under TTCP W-1) was set up to see how successfully various countries can deal with it. This KTA involved the simulation of the US Naval Ordnance Laboratory modified gap test and their underwater sensitivity test. For these tests, a large amount of experimental data was available. The explosive properties of H6 were made available to the various nations and they were asked to reproduce as well as possible the experimental data. Deficiencies in the detonation models would be uncovered by this process and areas for further work identified.

This work was performed at DREV between October 1996 and April 1997 under Project 2eb, Insensitive Munitions.

2.0 H6 EXPLOSIVE CHARACTERIZATION

The model used at DREV is called the Forest fire (FF) model. It has been described in detail by Mader (Ref. 1) and only parts of it will be briefly described. The model has

two components: an equation of state for the explosive and a description of the reaction rate.

The equation of state (EOS) for an explosive describes its pressure volume and temperature volume relationships as the detonation evolves. To do so, both the solid (unreacted) and gas (reacted) phases of the explosive are needed as well as rules for mixed (intermediate) states. The solid component of the explosive is described by basically the Grüneisen equation of state with a procedure for determining the temperature along the shock Hugoniot. The parameters which are needed to fully characterize it are: the unreacted shock Hugoniot ($U_S = C + S_{VN}u_p$), the initial density (ρ_o), and the Grüneisen gamma constant (γ_s , calculated from the isothermal compressibility (κ) which is the reciprocal of the bulk modulus, the coefficient of linear thermal expansion (α), the heat capacity (C_{V-s} and the density). All the experimental data for the explosive's properties were found in Ref. 2 (which are the same as the data supplied through the KTA). The initial temperature (T_o) and the initial pressure (P_o) are also needed but these are simply ambient conditions. The temperature is fitted to

$$\ln(T) = F_s + G_s(\ln v_s) + H_s(\ln v_s)^2 + I_s(\ln v_s)^3 + J_s(\ln v_s)^4.$$

The parameters used and the results of the fit are given in Table I.

The equation of state must also describe the gaseous reaction products. The original FF model used the isentrope through the Chapman-Jouget point as calculated by a chemical equilibrium computer program such as TIGER (Ref. 3). For the present work, the adiabat

TABLE IHOM solid parameters for H6

Parameter	Value
C	0.2832 cm μs^{-1}
S_{VN}	1.695
κ	1.35 10^{-10} Pa $^{-1}$
α	2.2 10^{-5} K $^{-1}$
C_{V-s}	2.67925430210E-01 cal g $^{-1}$ K $^{-1}$
ρ_o	1.76 g cm $^{-3}$
γ_s	2.47715333532E-01
T_o	300 K
P_o	10^{-6} MBar
F_s	-1.27429265631E+01
G_s	-1.02344211017E+02
H_s	-2.07188232489E+02
I_s	-1.78696324774E+02
J_s	-5.36968243009E+01

described by the experimental JWL parameters (Ref. 4) was used:

$$P = Ae^{-R_1 v_g/v_o} + Be^{-R_2 v_g/v_o} + C(v_g/v_o)^{-(1+\omega)}$$

However, a calculation was performed using TIGER to determine the temperature (T_{CJ}), the specific volume (v_{CJ}) and the heat capacity (C_{V-CJ}) at the CJ point and to set a zero point offset for the energy to be compatible with the solid EOS (using the large volume limit of the internal energy). The temperature along the isentrope is given by

$$T = T_o \left(\frac{v}{v_o} \right)^{-\omega}$$

where T_o is found by using the temperature and specific volume at the CJ point calculated by TIGER and v_o is the specific volume of the initial solid explosive. Some test simulations were performed, for the same situations, using both the TIGER (BKW) and the JWL EOS's.

TABLE II

HOM gaseous parameters

Parameter	Value
A	7.5807 MBar
B	0.08513 MBar
C	0.01143 MBar
R ₁	4.9
R ₂	1.1
ω	0.20
T _{CJ}	4887.6 K
v _{CJ}	0.4289 cm ³ g ⁻¹
C _{V-CJ}	0.525 cal g ⁻¹ K ⁻¹
Energy Offset	0.0575 MBar-cc

The final results were the same except at the highest pressures (greater than 15 GPa). For the rest of the simulations, the JWL EOS was used exclusively. The parameters are found in Table II.

With the EOS established, the rate constants for the explosive were then determined. Two things are needed: the reactive shock Hugoniot and the run-to-detonation versus impact pressure relation (the Pop plot). An estimate of the slope of reactive shock Hugoniot was made using

$$S = \frac{(D - C)}{(P_{CJ}/(\rho D))}$$

where D is the detonation velocity, C is the sound speed from the unreactive shock Hugoniot and P_{CJ} is the detonation pressure. A one dimensional test was simulated to verify if the experimental run-to-detonation versus impact pressure (the Pop plot, $\ln(\text{Run[cm]}) = \alpha_1 + \alpha_2 \ln(P[\text{MBar}])$) (Ref. 5) was reproduced. With the rate constants as initially

TABLE IIIFinal Forest fire rate coefficients

D	0.7490 cm μs^{-1}
P_{CJ}	0.245 MBar
C	0.2832 cm μs^{-1}
S	2.526
α_1	-4.872970903D0
α_2	-1.931620629D0
A_0	-10.078188326
A_1	317.85159600
A_2	-6251.1759687
A_3	84120.329723
A_4	-701812.53472
A_5	3493993.8682
A_6	-9476309.6034
A_7	10779937.824

calculated, it was not. Therefore, the (input) Pop plot was adjusted until agreement between the calculated and experimental Pop plot was more or less obtained (see Fig. 1 for the comparison). These improved rate constants were then used for subsequent simulations. Small improvements can be made to obtain better agreement but simulations with other modified rate coefficients showed that the results were not all that sensitive to further changes. The rates are fitted to the pressure:

$$\ln(\text{Rate}) = \sum_{i=0}^{i=7} A_i P^i.$$

The final input parameters and calculated rates are shown in Table III.

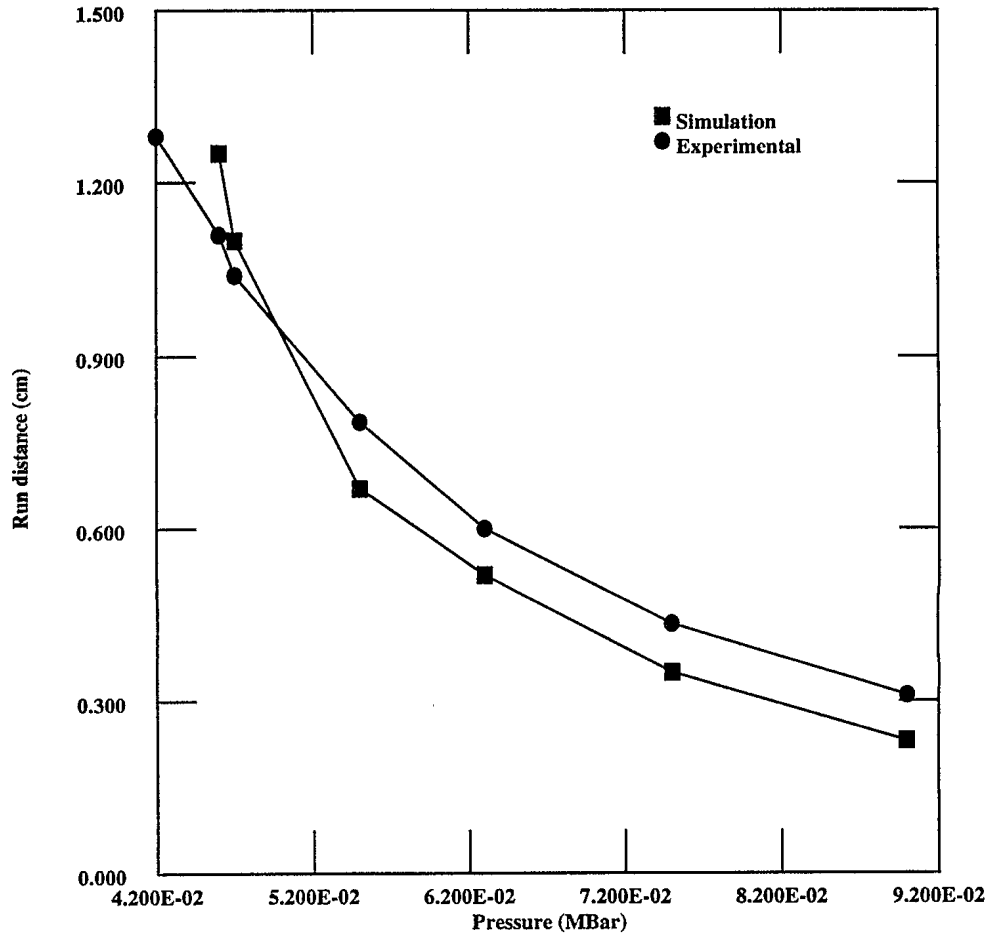


FIGURE 1 – Simulation of Pop plot experiment with modified coefficients

3.0 MODIFIED GAP TEST SIMULATIONS

The simulations were performed using DYNA2D to which the Forest fire model had been implemented. The setup had 50.8-mm diameter cylindrical symmetry. The 50.8-mm thick pentolite donor was modelled using a simple programmed burn with the detonation starting at the center of the bottom face at time zero and a JWL EOS for the reaction products (Ref. 4, DYNA2D parameters: ro 1.70, d 0.753, pcj 0.255, a 5.4094, b 0.093726, r1 4.5, r2 1.1, omega 0.35, e0 0.081, v0 1.0). The gap material polymethylmethacrylate (PMMA or plexiglas) was modelled as a kinematic-isotropic elastic-plastic material (material model 3 of DYNA, input parameters: ro 1.19, e 0.02170, pr 0.4, sigy .980e-3, etan 0.68563e-3, beta 1.0, hgqt 4, hgq 0.40, bqt 1, bqg 1.5, bql 0.06). The 12.7-mm thick H6 acceptor was modelled using the coefficients found in the previous section. The meshing was 10x65 (r-z) in the pentolite, 10 x n in the PMMA (where n is such that each element was 0.1 cm thick) and 10 x 32 in the H6. The simulations were run with gap thicknesses of 2.5, 3.0, 3.1, 3.2, 3.3, 3.5, 4.0, 4.5, 5.0 and 6.0 cm. The meshing is shown in Fig. 2.

For the analysis, the acceptor's maximum top surface velocity was plotted versus gap thickness. The results are shown in Fig. 3, as are the experimental results from Ref. 6. The typical input shock pulse is quasi-triangular but asymmetric, rising rapidly and falling more slowly with a full-width half-maximum of about 5 μ s. The critical gap thickness is about 29 mm in the simulations whereas the experiments found a critical thickness of about 32 mm which is fairly good agreement. In the simulations, this critical gap corresponds to a

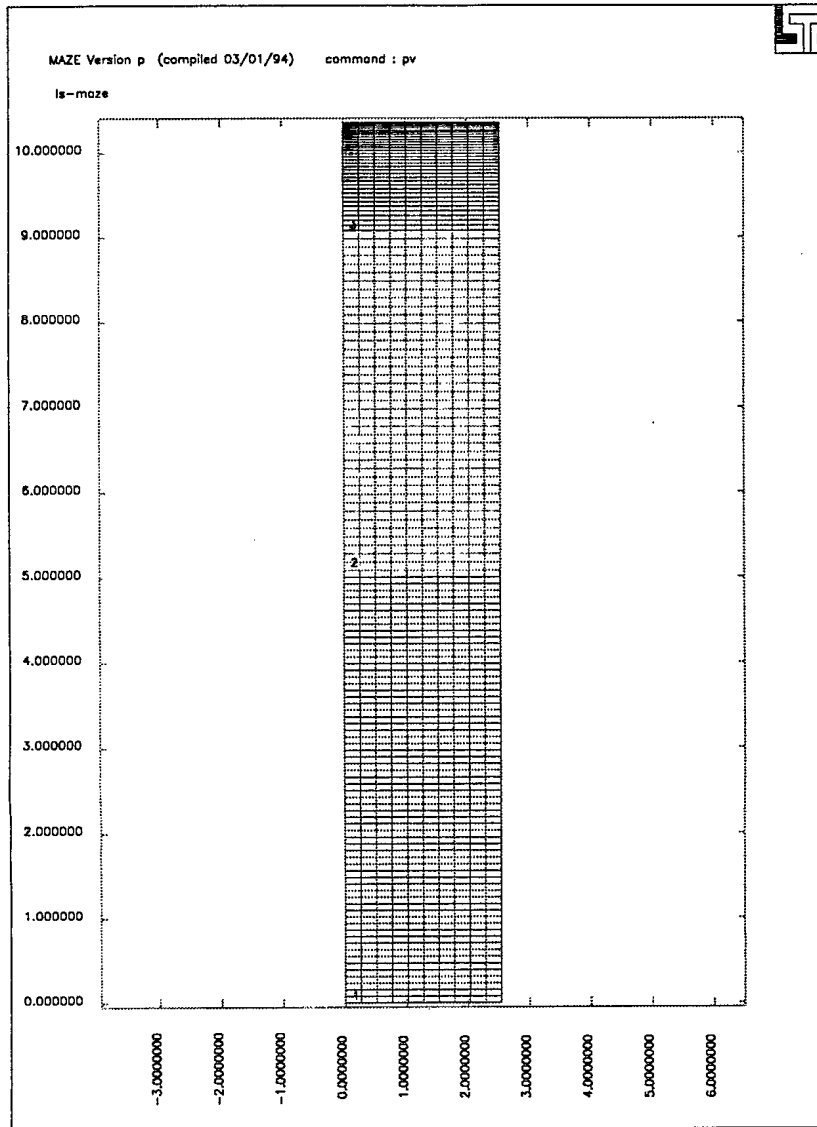


FIGURE 2 – Meshing used in PMMA gap test simulations (for a 4.0-cm gap). Along the vertical axis, the pentolite is between 0 and 5.08cm, the PMMA between 5.08 and 9.08 cm and the H6 between 9.08 and 10.35 cm.

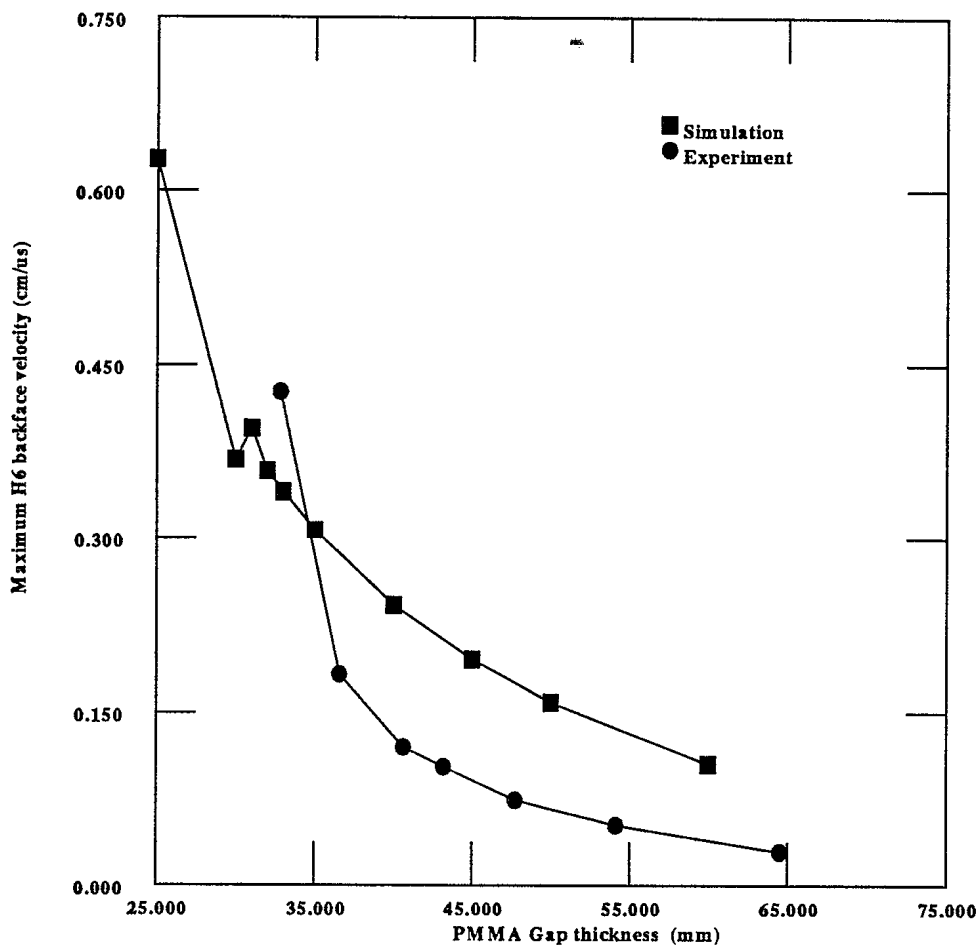


FIGURE 3 – Maximum backface velocity of H6 acceptor in PMMA gap test

pressure in the bottom center of the H6 disk of about 0.06 MBar. The velocities predicted by the simulations at large gap thicknesses are higher than those experimentally observed.

4.0 UNDERWATER SENSITIVITY TEST SIMULATIONS

The program DYNA2D was used to simulate the underwater sensitivity test (Ref. 6). A pentolite sphere (4.1-cm radius) was surrounded by water. A single disk of H6 (2.54-

cm radius, 1.27cm-thick) was placed at various distances (from 3.0 to 12.8 cm) from the outer surface of the sphere and was surrounded by water. The meshing used is shown in Fig. 4.

The pentolite was modelled with a programmed burn starting at its center and using a JWL equation of state for its reaction products as described in the previous section. The water was modelled hydrodynamically using a Grüneisen equation of state ($\rho = 1 \text{ g cm}^{-3}$, $C = 0.1647 \text{ cm } \mu\text{s}^{-1}$, and $S = 1.921$). The H6 was modelled as described earlier. The initial pressure applied to the explosive in the simulations agrees very well with the experimental pressure calculated for the underwater sensitivity test. In all cases, the pressure pulse as seen by the explosive was roughly triangular in shape with a full-width half-maximum of about $10 \mu\text{s}$. The velocity of the backsurface of the H6 disk was then followed. There was an initial backsurface velocity spike, steadily decreasing in about 30-40 microseconds to a steady-state velocity. The spike velocity was approximately twice the steady-state velocity. In Fig. 5, this steady-state top surface velocity is shown versus water gap thickness; the wider the water gap is, the lower the steady-state velocity is. There is also a critical gap thickness of roughly 50 mm (corresponding to a pressure of about 0.022 MBar in the bottom center element) below which the steady-state velocity rapidly rises. This is due to significant reaction and subsequent product gas generation in the explosive.

In the experimental case, it was found that the H6 was constantly expanding in thickness except for a few microseconds at the beginning. In the simulations, for cases

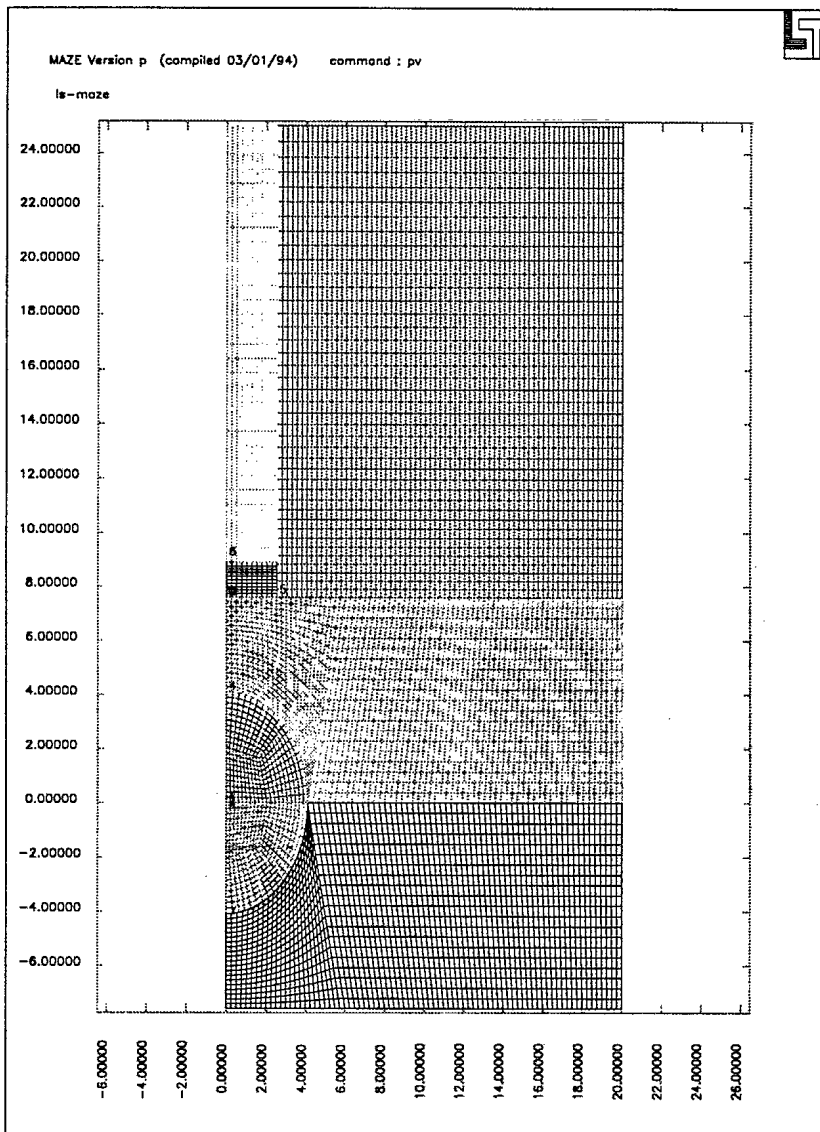


FIGURE 4 – Meshing used for the sympathetic detonation simulations (for a 3.5-cm water gap). Along the vertical axis, the pentolite is centered at (0,0) with a radius of 4.1cm, the H6 lies between 7.6 and 8.87 cm and everything else is water.

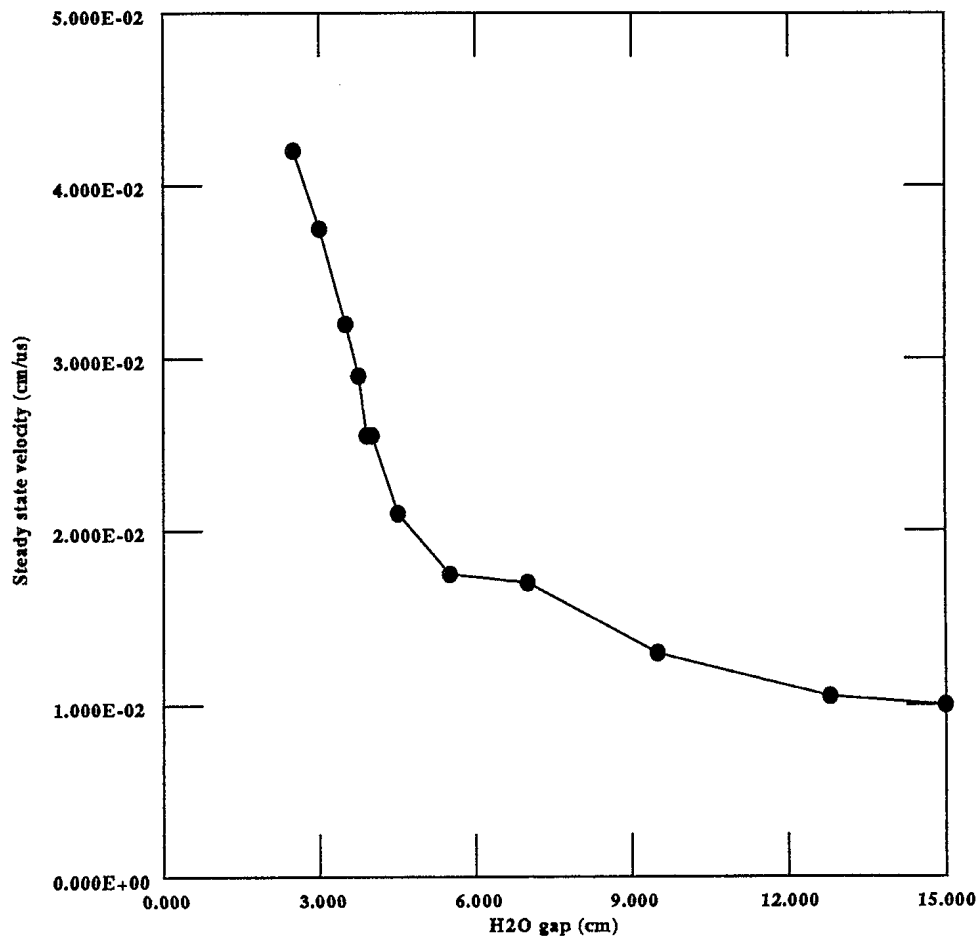


FIGURE 5 – Steady-state backface velocity of H6 acceptor in H₂O gap test

when there was an obvious reaction, this is indeed what is observed. However, when the reaction is weaker or not present, the disk spreads laterally, becoming flattened as it moves off and slowing slightly as it moves into the surrounding water.

5.0 COMMENTS ON THE RESULTS

There are two aspects to the results. The first aspect is the initial response of the explosive to the input shock. This seems to be modelled correctly. In the underwater sensitivity test, applied pressure pulses in the explosive acceptors were “quasi-triangular shaped” and with “pulse widths between 7 and 10 μs ” which is exactly what was found for the simulations. In the gap test, the applied pressure pulses had “half-widths at one-half peak stress from 1 to 2 μs ” whereas the simulations showed a bit longer interaction (5 μs). Also, from the experimental data, we know that the critical pressure for reaction is 3 times higher in the gap test than in the underwater test. This is confirmed by the simulations: 0.060 MBar in the gap test versus 0.022 MBar in the underwater test. In the gap test experiments, the critical pressure was 0.058 MBar, in excellent agreement with simulations.

The second aspect of results is the behaviour of the acceptors after the shock wave has struck. Qualitatively, the behaviour is correct: backsurface velocities which rise sharply below a critical gap (PMMA or water) thickness and which level off for thicker gaps. Quantitatively, there are problems. The simulations overestimate the velocities by factors of about 2 to 3. The reason for this difference is probably due to an inadequate equation of state for the explosive.

Overall, the results seem to indicate that the Forest fire model can be used to predict the initial onset of a detonation. However, with the solid-gas mixture EOS, behaviour afterwards is not well predicted. Simulations of practical problems will have to be run

twice: once to decide whether or not a given explosive in a specific geometry will ignite (using the FF model) and then, a second time, using either a solid EOS (e.g. Grüneisen) if there is no reaction or a gas EOS (e.g. JWL) model if there is a reaction, with an appropriately timed programmed burn. Reactions in which there is only partial reactions will be difficult to model accurately.

6.0 REFERENCES

1. Mader, C., "Numerical Modeling of Detonation", University of California Press, Berkeley, Calif., 1979.
2. Hall, T.N., Holden, J.R., "Navy Explosives Handbook", Naval Surface Warfare Center MP 88-116, October 1988, UNCLASSIFIED
3. Cowperthwaite, M., Zwisler, W.H., "TIGER Program Documentation", Stanford Research Institute, UNCLASSIFIED
4. Dobratz, B.M., Crawford, P.C., "LLNL Explosives Handbook", Lawrence Livermore National Laboratory UCRL-52997-Chg. 2, January 31 1985, UNCLASSIFIED
5. Hudson, L.C., "Computational Studies of Sympathetic Detonation between Two Axially Adjacent, Cased Charges of H6", in Schmidt, S.C. et al., "Shock Compression of Condensed Matter - 1991", Elsevier Science Publishers, Amsterdam, 1992.
6. Liddiard, T.P., Forbes, J.W., "A Summary Report of the Modified Gap Test and the Underwater Sensitivity Test", Naval Surface Warfare Center TR 86-350, 12 March 1987, UNCLASSIFIED



UNCLASSIFIED

INTERNAL DISTRIBUTION

DREV - TM - 9802

- 1 - Deputy Director General
- 1 - Chief Scientist
- 6 - Document Library
- 1 - Head, Weapons Effects Section
- 1 - Head, Energetic Materials Section
- 1 - Dr. G. McIntosh (author)
- 1 - Mr. P. Brousseau
- 1 - Dr. D. Nandlall
- 1 - Mr. M. Szymczak



UNCLASSIFIED

EXTERNAL DISTRIBUTION

DREV - TM - 9802

- 1 - DRDIM
- 1 - DRDIM (unbound copy)
- 1 - DRDB
- 1 - DSAL
- 1 - DSAL-2
- 1 - DAES
- 1 - DAES-3
- 1 - DFTEM-1
- 1 - DRES
Attn: Dr. J. Slater

- 1 - Dr. W.H. Wilson
Naval Surface Warfare Center - Indian Head Div.
101 Strauss Ave.
Indian Head, Md 20640-5035
USA

- 1 - Dr. P.J. Haskins
DRA Fort Halstead
Sevenoaks, Kent TN14 7BP
United Kingdom

- 1 - Dr. David A. Jones
Weapons Systems Division
Aeronautical and Maritime Research Laboratory
PO Box 4331, Victoria 3001
AUSTRALIA

- 1 - Dr. Ries Verbeek
TNO Prins Maurits Laboratorium
Postbus 45
2280AA Rijswijk ZH
Netherlands

- 1 - NIMIC
NATO Headquarters
B-1110 Brussels
Belgium



UNCLASSIFIED
SECURITY CLASSIFICATION OF FORM
(Highest classification of Title, Abstract, Keywords)

DOCUMENT CONTROL DATA

1. ORIGINATOR (name and address) Defence Research Establishment Valcartier 2459 Pie-XI Blvd. North Val-Belair, Qc G3J 1X5 Canada		2. SECURITY CLASSIFICATION (Including special warning terms if applicable) Unclassified	
3. TITLE (Its classification should be indicated by the appropriate abbreviation (S,C,R or U)) Modelling of the Explosive H6			
4. AUTHORS (Last name, first name, middle initial. If military, show rank, e.g. Doe, Maj. John E.) McIntosh, G.			
5. DATE OF PUBLICATION (month and year) March 1998		6a. NO. OF PAGES 17	6b. NO. OF REFERENCES 6
7. DESCRIPTIVE NOTES (the category of the document, e.g. technical report, technical note or memorandum. Give the inclusive dates when a specific reporting period is covered.) technical memorandum			
8. SPONSORING ACTIVITY (name and address)			
9a. PROJECT OR GRANT NO. (Please specify whether project or grant) Project 2eb, Insensitive Munitions		9b. CONTRACT NO.	
10a. ORIGINATOR'S DOCUMENT NUMBER DREV-TM-		10b. OTHER DOCUMENT NOS. N/A	
11. DOCUMENT AVAILABILITY (any limitations on further dissemination of the document, other than those imposed by security classification) <input checked="" type="checkbox"/> Unlimited distribution <input type="checkbox"/> Contractors in approved countries (specify) <input type="checkbox"/> Canadian contractors (with need-to-know) <input type="checkbox"/> Government (with need-to-know) <input type="checkbox"/> Defence departments <input type="checkbox"/> Other (please specify) :			
12. DOCUMENT ANNOUNCEMENT (any limitation to the bibliographic announcement of this document. This will normally correspond to the Document Availability (11). However, where further distribution (beyond the audience specified in 11) is possible, a wider announcement audience may be selected.)			

UNCLASSIFIED

SECURITY CLASSIFICATION OF FORM

13. **ABSTRACT** (a brief and factual summary of the document. It may also appear elsewhere in the body of the document itself. It is highly desirable that the abstract of classified documents be unclassified. Each paragraph of the abstract shall begin with an indication of the security classification of the information in the paragraph (unless the document itself is unclassified) represented as (S), (C), (R), or (U). It is not necessary to include here abstracts in both official languages unless the text is bilingual).

An attempt to model the shock-to-detonation behaviour of the explosive H-6 has been made. The Forest fire model of ignition was calibrated using experimental data. Simulations of Plexiglas and water gap tests were then made using DYNA2D into which the Forest fire model had been implemented. The results show that while the onset of detonation (critical gap thickness) can be predicted fairly well, the subsequent events, such as backsurface velocities of the explosive, are not accurately predicted.

14. **KEYWORDS, DESCRIPTORS or IDENTIFIERS** (technically meaningful terms or short phrases that characterize a document and could be helpful in cataloguing the document. They should be selected so that no security classification is required. Identifiers, such as equipment model designation, trade name, military project code name, geographic location may also be included. If possible keywords should be selected from a published thesaurus. e.g. Thesaurus of Engineering and Scientific Terms (TEST) and that thesaurus-identified. If it is not possible to select indexing terms which are Unclassified, the classification of each could be indicated as with the title.)

explosives
H-6
finite element analysis
DYNA-2D
detonation
sea mines

#507638

UNCLASSIFIED

SECURITY CLASSIFICATION OF FORM